Supporting Information

Atmospheric pressure single photon laser ionization (APSPLI) mass spectrometry using a 157 nm fluorine excimer laser for sensitive and selective detection of non- to semi-polar hydrocarbons

Christopher P. Rüger^{1,2*#}, Anika Neumann^{1,2#}, Martin Sklorz³, Ralf
Zimmermann^{1,2,3}

1 Joint Mass Spectrometry Centre, Chair of Analytical Chemistry, University of Rostock, 18059 Rostock, Germany

2 Department Life, Light & Matter (LLM), University of Rostock, 18051 Rostock, Germany
3 Joint Mass Spectrometry Centre, Cooperation Group "Comprehensive Molecular Analytics"

(CMA), Helmholtz Zentrum München (HMGU), 85764 Neuherberg, Germany

Keywords: atmospheric pressure laser ionization (APLI), excimer laser, high-resolution mass spectrometry, polycyclic aromatic hydrocarbons (PAH), gas chromatography

^{*} corresponding author, christopher.rueger@uni-rostock.de

[#] these authors contributed equally to the manuscript

Table of Content

Table S1: Composition of the A4 polycyclic aromatic hydrocarbon standard mixture. Structure, concentration, molecular formula and exact mass are given.

Table S2: Composition of the M3 polycyclic aromatic hydrocarbon standard mixture. Structure, concentration, molecular formula and exact mass are given.

Figure S1: Photographic image of the atmospheric pressure single photon laser ionization (APSPLI) setup using a fluorine excimer laser (157 nm). The Nd:YAG solid state laser operated at the 4th harmonic (266 nm) for APLI is also depicted.

Figure S2: Atmospheric pressure single-photon laser ionization (APSPLI) of Indeno[1,2,3,*c*,*d*]pyrene subjected to the source by gas chromatography coupling. Aside from the characteristic oxidation ionization artifact [M+O]^{+•}, doubly charged species [M+O]^{2+•} can particularly be found for species with high aromaticity (high DBE).

Figure S3: Effect of deploying an oxygen-, a water-filter, and both filter types for purification of the nebulizer gas supply to the relative occurrence of the oxidized ionization artifact [M+O]*+ compared to the molecular radical cation [M]*+.

Figure S4: Visualizing the variation of the laser beam position (diameter ~7 mm). Schematic cut through the ionization chamber with evolved gas analysis (EGA) exhaust at the left and mass spectrometric inlet at the right. Laser beam position a) near the sample (EGA) introduction, b) in the middle of the ion source, and c) close to the mass spectrometry entrance.

Figure S5: Selected compounds of the PAH standard mixture ionized by APSPLI at different positions in the ion source. The intensity of the radical cations (depicted at the ordinate) strongly depends on the ionization location.

Figure S6: Compound class distribution of the light crude oil introduced by GC and ionized by APSPLI. The classes are divided into the respective radical cation (odd-electron configuration) and protonated species (even-electron configuration). Primarily radical cations could be found with a factor of 60-180 higher abundances compared to the protonated species.

Figure S7: Double bond equivalent (DBE) distribution for the CH-, CHO-, CHS- and CHSO-class. The pattern between the CHO- and CH- as well as between CHS- and CHSO-class significantly differ indicating a rather low contribution of oxidized ionization artifacts.

Figure S8: Gas chromatography atmospheric pressure single photon laser ionization (APSPLI,GC-APSPLI at 157 nm of a light crude oil (CPC Blend, Kazakhstan). a) CH₂-based Kendrick mass defect plot color-coded according to the attributed compound class and size coded according to the summed abundance, and b) mass spectrometric enlargement to the nominal mass 360 with attributed elemental compositions.

Table S1: Composition of the A4 polycyclic aromatic hydrocarbon standard mixture. Structure, concentration, molecular formula and exact mass are given.

#	Structure	Name, sum formula, exact mass	Concentration [mg/l]
1		Naphthalene	7.65
		C ₁₀ H ₈	
		128.062600	
2		Biphenyl	1.95
		C ₁₂ H ₁₀	
		154.078250	
3		Acenapthene	7.96
		C ₁₂ H ₁₀	
		154.078250	
4		Fluorene	9.21
		C ₁₃ H ₁₀	
		166.078250	
5		Phenanthrene	8.57
		C ₁₄ H ₁₀	
		178.078250	
6		Anthracene	8.08
		C ₁₄ H ₁₀	
		178.078250	
7		Fluoranthene	7.72
		C ₁₆ H ₁₀	
		202.078250	
8		Pyrene	9.22
		C ₁₆ H ₁₀	
		202.078250	
9		Benz[a]anthracene	1.26
		C ₁₈ H ₁₂	
		228.093900	
10		Chrysene	1.65
		C ₁₈ H ₁₂	-
		228.093900	
11		Benzo[<i>e</i>]pyrene	1.77
		C ₂₀ H ₁₂	,
		252.093900	
12		Perylene	1.48
12		C ₂₀ H ₁₂	1.70
		252.093900	
12			1.42
13		Coronene	1.43
		C ₂₄ H ₁₂	
		300.093900	

Table S2: Composition of the M3 polycyclic aromatic hydrocarbon standard mixture. Structure, concentration, molecular formula and exact mass are given.

#	Structure	Name, sum formula, exact mass	Concentration [mg/l]
1		Naphthalene	4.95
		C ₁₀ H ₈	
	V V	128.062600	
2		Acenaphtylene	4.38
		C ₁₂ H ₈	
		152.062600	
3		Biphenyl	0.77
		C ₁₂ H ₁₀ 154.078250	
4		Acenapthene	4.89
		C ₁₂ H ₁₀	
		154.078250	
5		Fluorene	5.53
		C ₁₃ H ₁₀	
6		166.078250 Phenanthrene	4.76
		$C_{14}H_{10}$	4.70
		178.078250	
7		Anthracene	1.30
		C ₁₄ H ₁₀	
		178.078250	1.70
8		Fluoranthene C ₁₆ H ₁₀	1.70
		202.078250	
	× //		
9		Pyrene	2.37
		C ₁₆ H ₁₀	
		202.078250	
10		2-Phenylnaphthalene	0.76
		C ₁₆ H ₁₂	
		204.093900	
11	· · ·	Benz[a]anthracene	1.69
		$C_{18}H_{12}$	1.03
		228.093900	
12		Chrysene	1.64
		C ₁₈ H ₁₂	1.01
		228.093900	
13		Benzo[c]phenanthrene	0.78
		(3,4-Benzophenanthrene) C ₁₈ H ₁₂	
		228.093900	
	i e e e e e e e e e e e e e e e e e e e	The state of the s	1

14	<u></u>	Benzo[b]fluoranthene	0.60
14		$C_{20}H_{12}$	0.00
		252.093900	
15		Benzo[k]fluoranthene	0.86
		C ₂₀ H ₁₂	
		252.093900	
16		Benzo[a]pyrene	0.78
		C ₂₀ H ₁₂	
		252.093900	
17		Benzo[e]pyrene	0.81
		$C_{20}H_{12}$	
		252.093900	
18		Perylene	0.43
		C ₂₀ H ₁₂	
		252.093900	
19		2,2'-Binaphthyl	0.77
		C ₂₀ H ₁₄	
		254.109550	
20		Indeno[1,2,3, <i>c</i> , <i>d</i>]pyrene	0.41
		C ₂₂ H ₁₂ 276.093900	
		270.033300	
21		Benzo[<i>g,h,i</i>]perylene	0.42
		$C_{22}H_{12}$	
		276.093900	
22		Dibenz[a,h]anthracene	0.43
		C ₂₂ H ₁₄	
		278.109550	
23		Picene	0.33
		C ₂₂ H ₁₄	
		278.109550	
24		Dibenz[a,c]anthracene	0.74
		(1,2,3,4-Dibenzanthracene)	
		C ₂₂ H ₁₄	
		278.109550	
25		Coronene	0.44
		C ₂₄ H ₁₂	
		300.093900	
26	O _{II}	Methyl eicosanoate	0.70
	CH ₃ (CH ₂) ₁₇ CH ₂ OCH ₃	CH ₃ (CH ₂) ₁₈ COOCH ₃	
		326.318480	

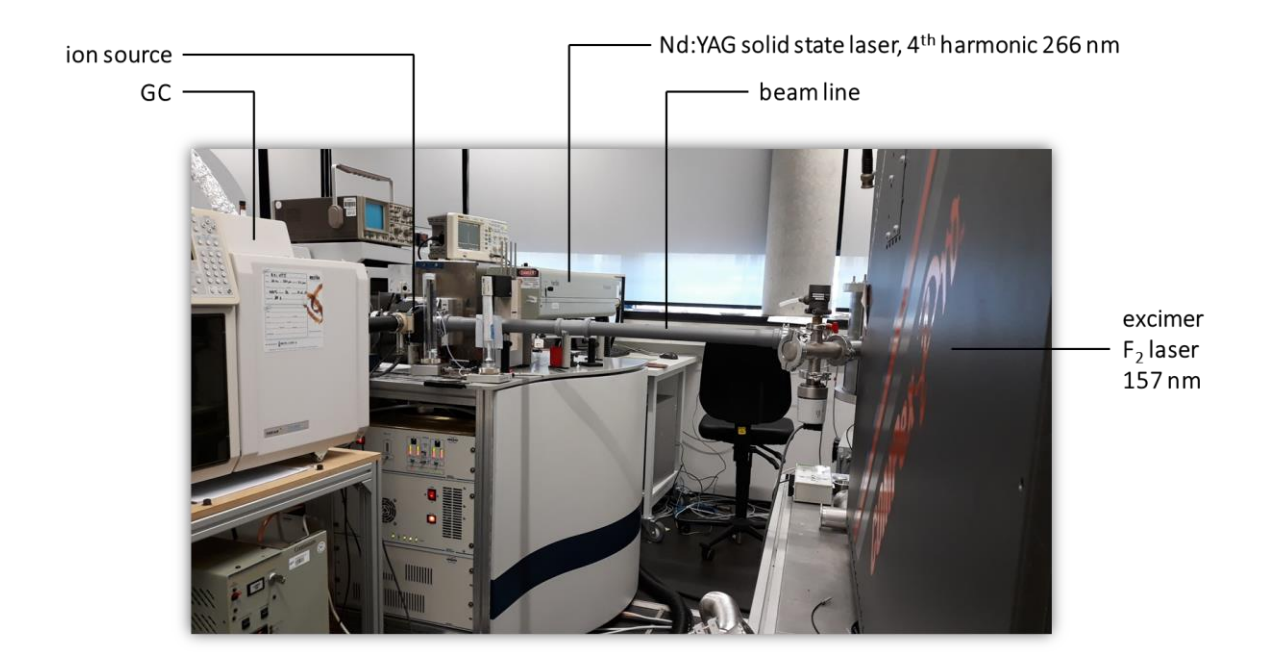


Figure S1: Photographic image of the atmospheric pressure single photon laser ionization (APSPLI) setup using a fluorine excimer laser (157 nm). The Nd:YAG solid state laser operated at the 4th harmonic (266 nm) for APLI is also depicted.

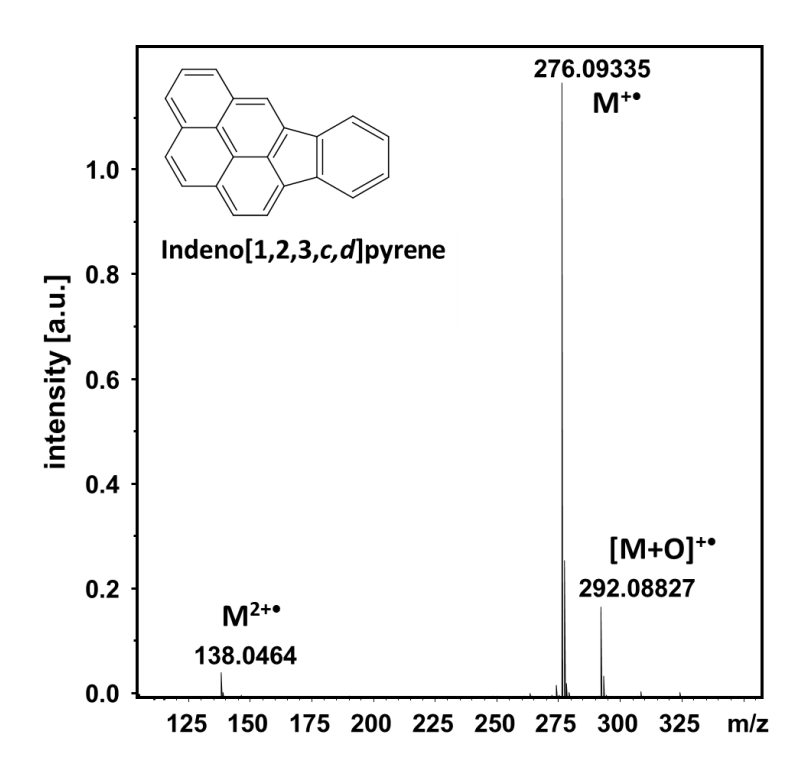


Figure S2: Atmospheric pressure single-photon laser ionization (APSPLI) of Indeno[1,2,3,*c*,*d*]pyrene subjected to the source by gas chromatography coupling. Aside from the characteristic oxidation ionization artifact [M+O]^{+•}, doubly charged species [M+O]^{2+•} can particularly be found for species with high aromaticity (high DBE).

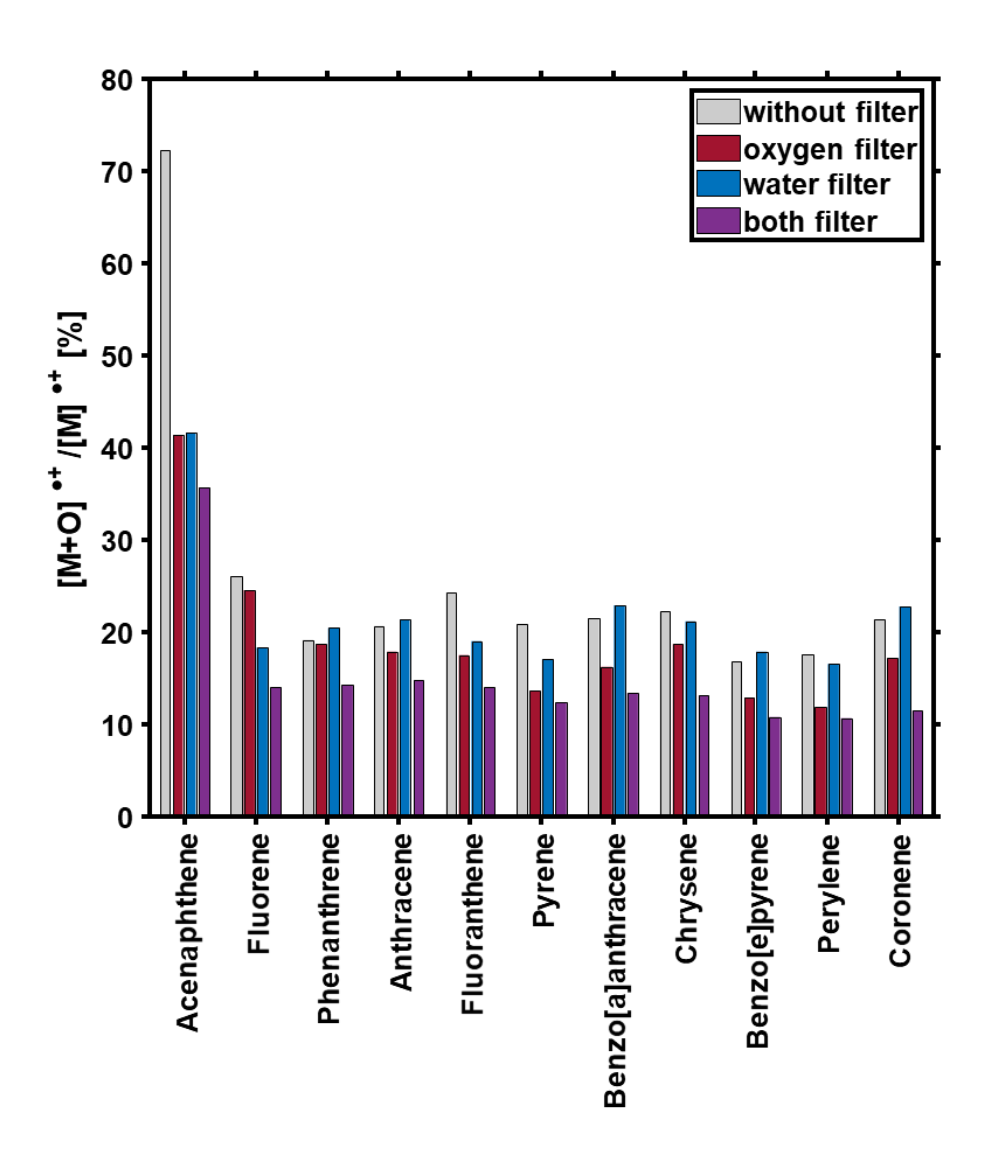


Figure S3: Effect of deploying an oxygen-, a water-filter, and both filter types for purification of the nebulizer gas supply to the relative occurrence of the oxidized ionization artifact [M+O]*+ compared to the molecular radical cation [M]*+.

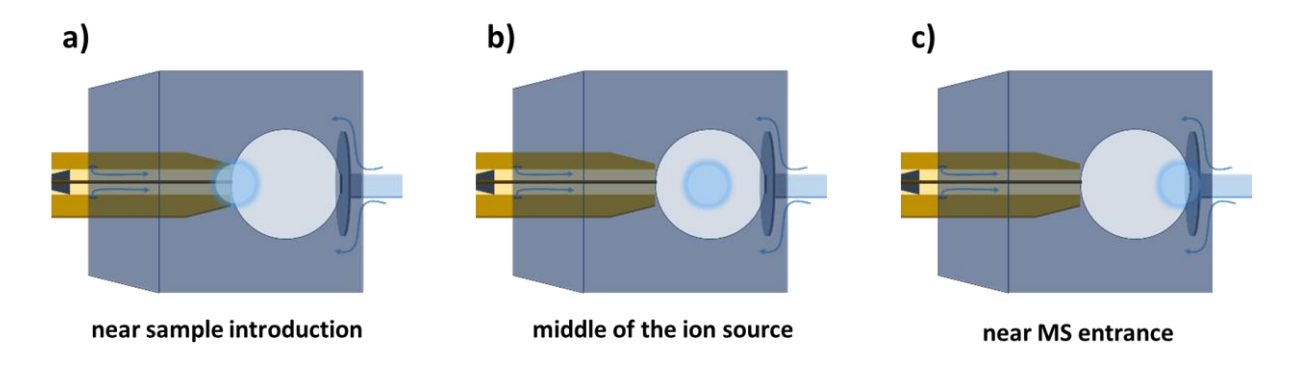


Figure S4: Visualizing the variation of the laser beam position (diameter ~7 mm). Schematic cut through the ionization chamber with evolved gas analysis (EGA) exhaust at the left and mass spectrometric inlet at the right. Laser beam position a) near the sample (EGA) introduction, b) in the middle of the ion source, and c) close to the mass spectrometry entrance.

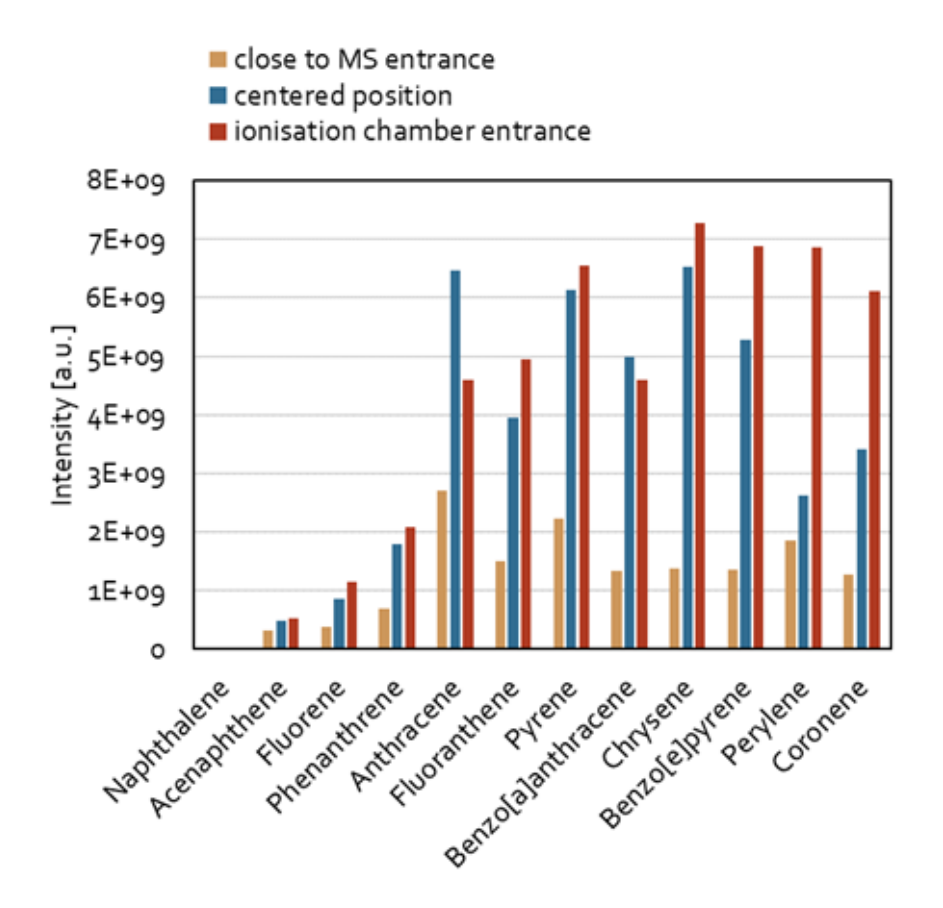


Figure S5: Selected compounds of the PAH standard mixture ionized by APSPLI at different positions in the ion source. The intensity of the radical cations (depicted at the ordinate) strongly depends on the ionization location.

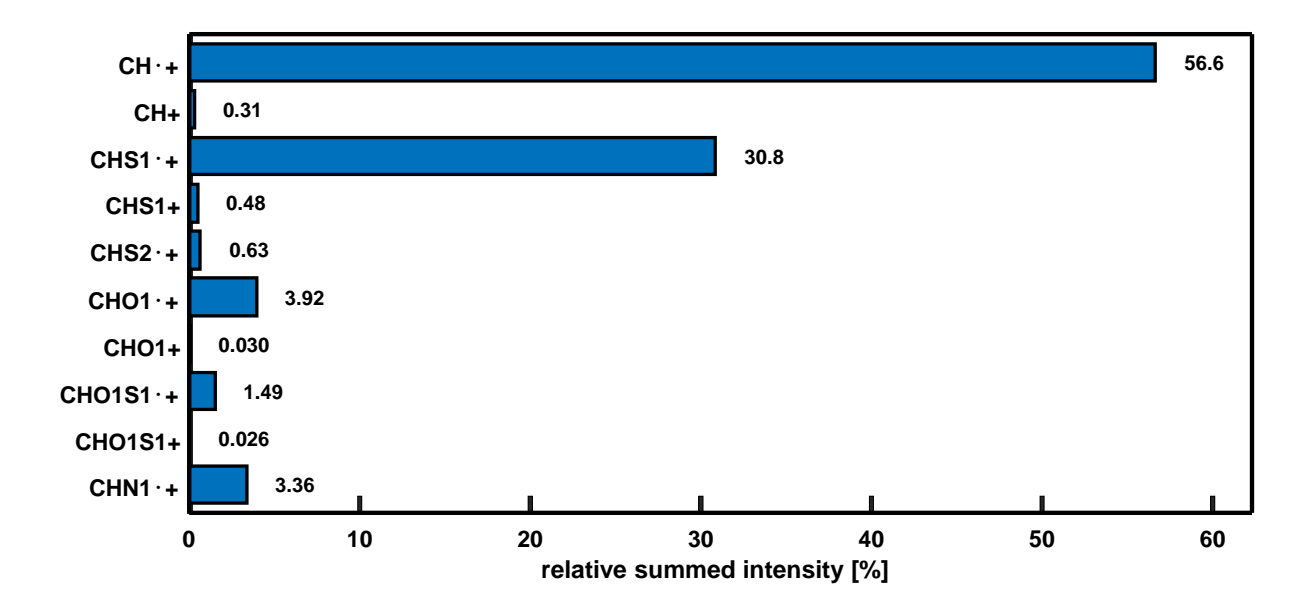


Figure S6: Compound class distribution of the light crude oil introduced by GC and ionized by APSPLI. The classes are divided into the respective radical cation (odd-electron configuration) and protonated species (even-electron configuration). Primarily radical cations could be found with a factor of 60-180 higher abundances compared to the protonated species.

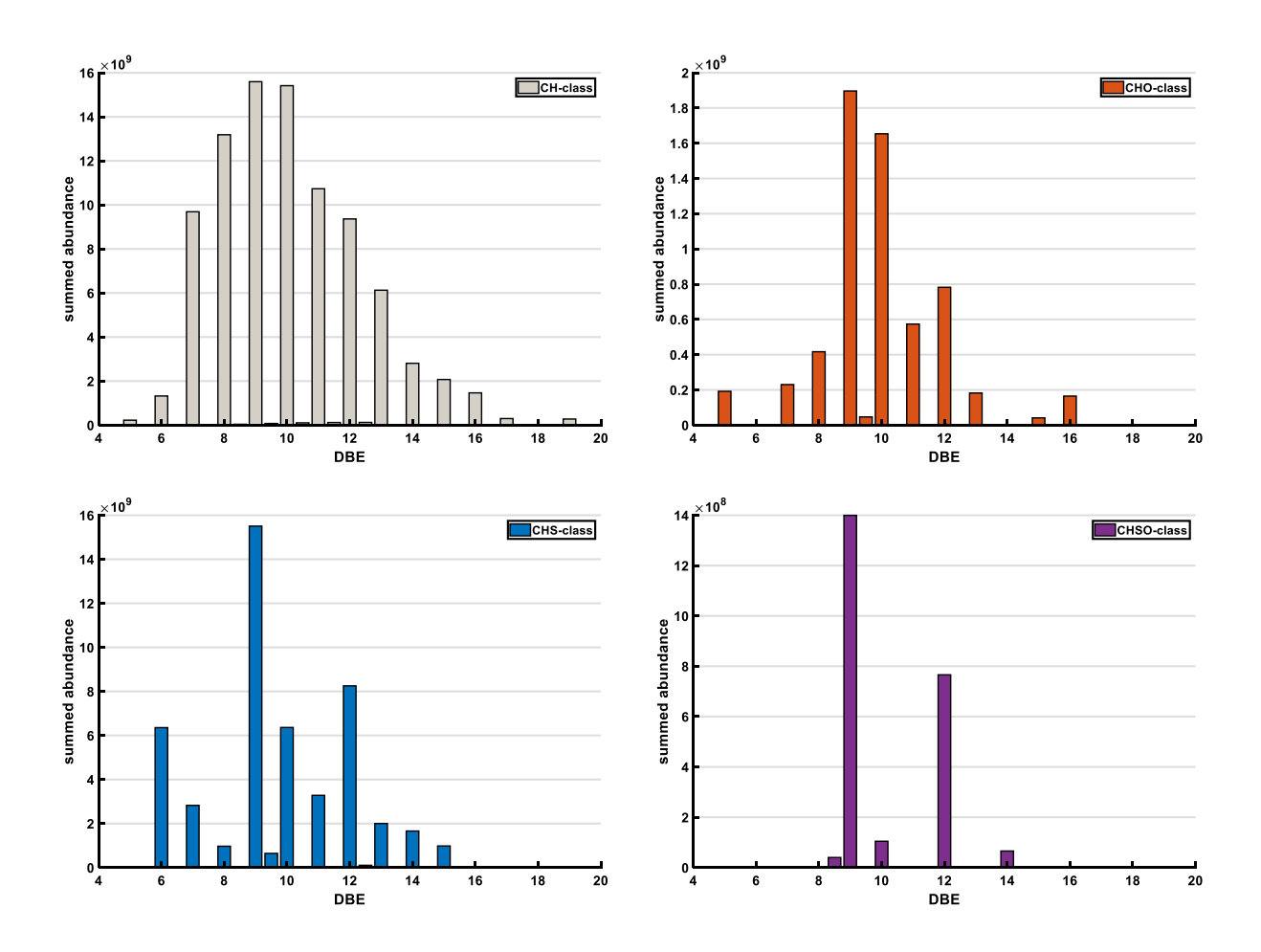


Figure S7: Double bond equivalent (DBE) distribution for the CH-, CHO-, CHS- and CHSO-class. The pattern between the CHO- and CH- as well as between CHS- and CHSO-class significantly differ indicating a rather low contribution of oxidized ionization artifacts.

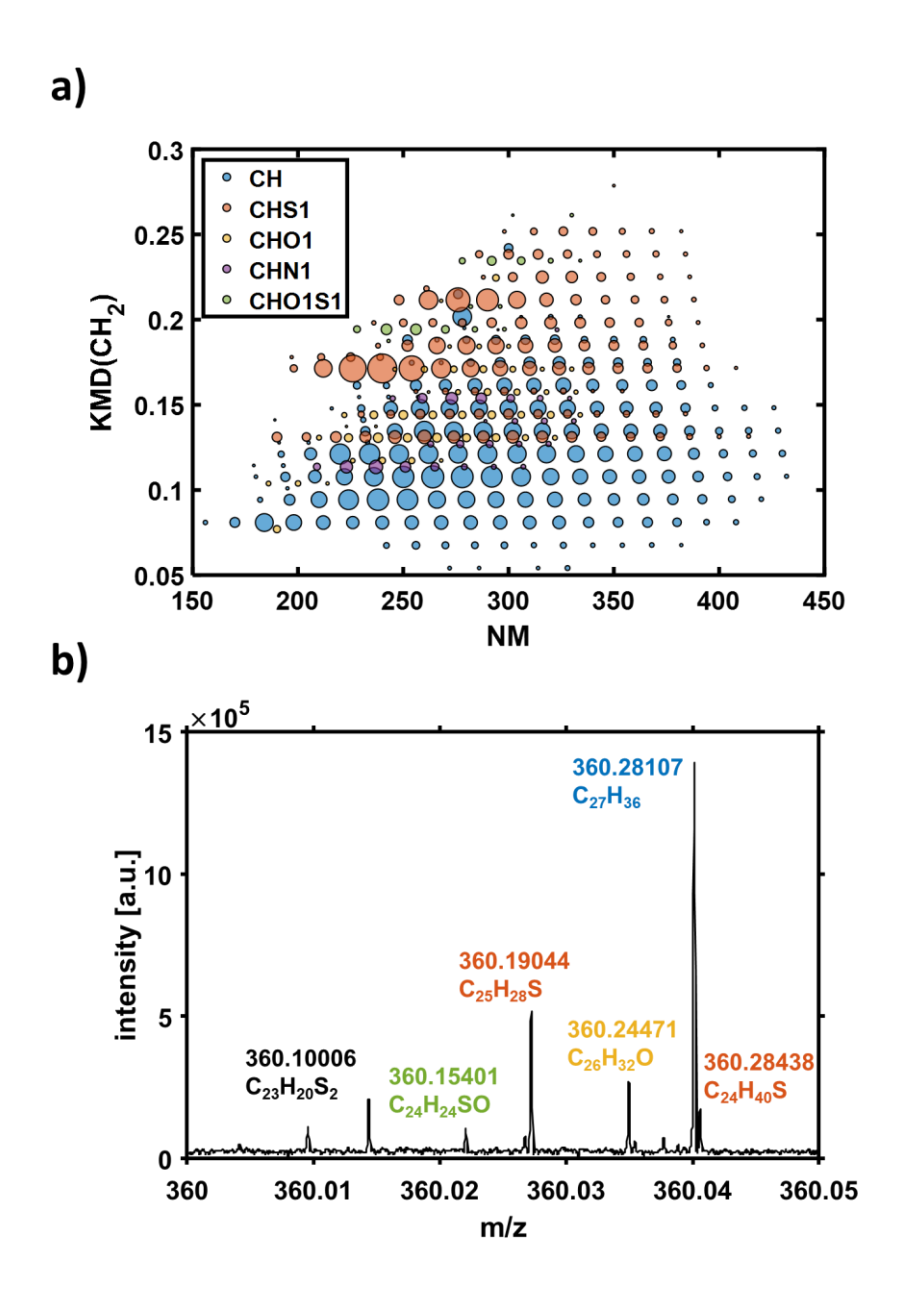


Figure S8: Gas chromatography atmospheric pressure single photon laser ionization (GC-APSPLI) at 157 nm of a light crude oil (CPC Blend, Kazakhstan). a) CH₂-based Kendrick mass defect plot color-coded according to the attributed compound class and size coded according to the summed abundance, and b) mass spectrometric enlargement to the nominal mass 360 with attributed elemental compositions.